Differential Extractability of Influenza Virus Hemagglutinin During Intracellular Transport in Polarized Epithelial Cells and Nonpolar Fibroblasts

Jeanne E. Skibbens,*‡ Michael G. Roth,§ Karl S. Matlin‡

* Verna and Marrs McLean Department of Biochemistry, Baylor College of Medicine, Houston, Texas 77030;
‡ Department of Anatomy and Cellular Biology, Harvard Medical School, Boston, Massachusetts 02115; and
§ Department of Biochemistry, University of Texas Health Science Center at Dallas, Dallas, Texas 35235

Abstract. Biochemical changes in the influenza virus hemagglutinin during intracellular transport to the apical plasma membrane of epithelial cells were investigated in Madin-Darby canine kidney (MDCK) cells and in LLC-PK1 cells stably transfected with a hemagglutinin gene. After pulse-labeling a substantial fraction of hemagglutinin was observed to become insoluble in isotonic solutions of Triton X-100. Insolubility of hemagglutinin was detected late in the transport pathway after addition of complex sugars in the Golgi complex but before insertion of the protein in the plasma membrane. Insolubility was not dependent on oligosaccharide modification since deoxymannojirimycin (dMM), which inhibits mannose trimming, failed to prevent its onset. Insolubility was not due to assembly of virus particles at the plasma membrane because insoluble hemagglutinin was also observed in transfected cells. Hemagglutinin insolubility was also seen in MDCK cells cultured in suspension and in chick embryo fibroblasts, indicating that insolubility and plasma membrane polarity are not simply correlated. In addition to insolubility, an apparent transport-dependent reduction of the disulfide bond linking HA1 and HA2 in hemagglutinin was detected. Because of the timing of both insolubility and the loss of the disulfide bond, these modifications may be important in the delivery of the hemagglutinin to the cell surface.

In eukaryotic cells, integral plasma membrane proteins are synthesized on membrane-bound polyribosomes of the rough endoplasmic reticulum and transported through the Golgi apparatus to their final destinations. In polarized epithelial cells this process is more complex because the plasma membrane is organized into apical and basolateral domains. Each domain has a unique protein and lipid composition achieved by sorting membrane components. How sorting occurs is not understood and is one of the most challenging problems in cell biology.

When Madin-Darby canine kidney (MDCK) cells, a polarized epithelial cell line (10, 50), are infected with enveloped RNA viruses, new virions bud exclusively from either the apical or basolateral plasma membrane. Influenza virus, for example, matures from the apical plasma membrane while vesicular stomatitis virus buds basolaterally (43). Budding from the apical or basolateral domain is dependent on polar insertion of the viral glycoproteins. The influenza proteins hemagglutinin and neuraminidase are concentrated on the apical plasma membrane while vesicular stomatitis virus G protein is mainly localized to the basolateral surface in infected cells (42). Sorting of viral glycoproteins is not dependent on the viral infection; epithelial cells expressing hemagglutinin or G protein without other viral proteins still insert these proteins into the correct domain (46, 52). Instead, the viral proteins apparently possess structural features recognized by the cellular sorting machinery.

Previous studies have delineated the transport pathways for apical and basolateral viral glycoproteins in MDCK cells. Hemagglutinin has been colocalized with G protein throughout the transport pathway to the *trans*-Golgi (9, 32, 39, 42). Beyond the *trans*-Golgi, the apical and basolateral pathways diverge such that hemagglutinin and G protein are directly inserted in their correct plasma membrane domains (21, 25, 36, 40). Similarly, direct pathways have been reported for endogenous MDCK cell proteins (6, 11, 18).

The finding that apical and basolateral transport pathways in MDCK cells diverge between the Golgi complex and the cell surface suggests that sorting is a Golgi function. The precise site where sorting occurs may be a specialized part of the *trans*-Golgi called the *trans*-Golgi network (13). The *trans*-Golgi network, in fact, may be a crossroads for membrane traffic in the cell where proteins destined for diverse pathways are segregated into vesicles for delivery (13, 14, 16, 32-34, 55).

From the work with MDCK cells it is evident that the mechanism of intracellular transport and sorting of membrane glycoproteins are closely related events. In this paper

these problems are addressed by looking for biochemical changes in the influenza hemagglutinin that occur late in the transport pathway during delivery of the protein to the plasma membrane. It is demonstrated that alterations in hemagglutinin occur that cause it to become insoluble in a nonionic detergent as it exits from the Golgi complex. In addition, an apparent loss of a disulfide bond during transport is observed. Each of these modifications may be important in the delivery of the hemagglutinin to the cell surface in both polarized and nonpolarized cells.

Materials and Methods

Materials

Tissue culture cells were grown on Falcon plastics in growth media from Gibco Laboratories, Grand Island, NY. Nonionic detergents for extracting the cells were, Triton X-100 (Sigma Chemical Co., St. Louis, MO), Surfact-Amps Purified Triton X-100 (Pierce Chemical Co., Rockford, IL), and NP-40 (Sigma Chemical Co.).

Cells and Viruses

MDCK cells exhibiting low transmonolayer resistance (MDCK II) were used (50). Stock and experimental cells were cultured as previously described (20).

MDCK cells were prepared for suspension culture by trypsinizing subconfluent stock cells and suspending them in media specially formulated for suspension culture (S-MEM) supplemented with dialyzed 5% FBS, 10 mM Hepes, pH 7.3, penicillin, and streptomycin. MDCK cells were cultured in suspension for 36 h in siliconized spinner flasks at a density of 1×10^5 cells/ml.

Experiments with LLC-PK1 cells expressing hemagglutinin were performed with a continuous cell line that stably maintains a bovine papilloma virus vector containing the cDNA for the A/Japan/305/57 hemagglutinin (H2 subtype; PKHA cells). PKHA cell stocks were grown in 75-cm^2 flasks in high glucose (4.5 g/liter) Dulbecco's MEM supplemented with 10% FBS, penicillin, and streptomycin until confluent (~4 d). Stock cells were subcultured approximately once a week at a dilution of 1:5. For experiments, PKHA cells were grown on Millicell-HA filters (30 mm, pore size 0.45 μm; Millipore Corp., Bedford, MA). A confluent flask of PKHA cells was trypsinized and the cells were suspended in 50 ml growth medium. A 3-ml aliquot of the cell suspension was placed on each filter and the cells were cultured for 4 d.

Chick embryo fibroblasts (CEF)[1] were prepared with 11-d chick embryos. The cells were suspended in high glucose Dulbecco's MEM supplemented with 10% FBS, penicillin, and streptomycin. The cell cultures were expanded to 75-cm^2 flasks and confluent flasks were divided into 40 35-mm plates for use in pulse-chase experiments.

For most experiments influenza virus A/PR/8/34 (H1 subtype; PR8), plaque purified on MDCK cells, was used. Viral stocks were grown in 10-d embryonated chicken eggs, concentrated by centrifugation, and titered on MDCK cells as previously described (22). Typical titers were from 10^{10}–10^{11} plaque-forming units/ml.

Influenza ts61S mutant (WSN subtype) was used to visualize hemagglutinin transport by immunofluorescence. Stocks of ts61S were grown from individual plaques picked up from MDCK cell monolayers as previously described (23).

Antibodies

A polyclonal antiserum against the PR8 hemagglutinin was raised in rabbits as previously described (22). The antiserum reacted against both hemagglutinin and the capsid protein NP. To enrich for hemagglutinin specific antibodies the antiserum was passed over an affinity column of ~1.3 mg hemagglutinin coupled to 0.35 g CNBr-Sepharose (Pharmacia Fine Chemicals, Piscataway, NJ). The affinity-purified antibodies were stored at −20°C in 50% (vol/vol) glycerol/PBS. Affinity purification reduced reactivity with NP, but did not eliminate it.

The monoclonal antibodies H28-E23 and H15-E8 141 against hemagglutinin were obtained from W. Gerhart and J. Yewdell of the Wistar Institute, Philadelphia, PA. To immunoprecipitate the PR8 hemagglutinin, H28-E23 antibodies were used either as culture supernatants or antibodies were purified from the culture supernatants by affinity chromatography on protein A–Sepharose (Pharmacia Fine Chemicals). For affinity chromatography, culture supernatants were passed over the protein A–Sepharose column then eluted with low pH (0.1 M citrate pH 3.0). Peak fractions were immediately neutralized with 1 M Tris base, dialyzed against 50% (vol/vol) glycerol/PBS, and stored at −20°C. The H15-E8 141 monoclonal specific for the WSN subtype of hemagglutinin, was used as undiluted culture supernatant for immunofluorescence.

For immunoprecipitation of hemagglutinin from PKHA cells, rabbit polyclonal serum against the H2 hemagglutinin was used. The antiserum was provided by M.-J. Gething (University of Texas, Southwestern Medical School, Dallas, TX).

Radiolabeling and Extraction

MDCK cells grown on 35-mm plates were infected and pulse-labeled as previously described (20) except all incubations were performed on a waterbath and the media were supplemented with 0.035% (wt/vol) sodium bicarbonate for pH stability.

To separate soluble and insoluble fractions, the cells were extracted with 1.0 ml of extraction buffer, consisting of 25 mM Hepes, pH 7.4, 0.15 M NaCl, 1% (wt/vol) Triton X-100, and a protease inhibitor cocktail (10 μg/ml aprotinin, 1 mM PMSF, 17 μg/ml benzamidine, 1 μg/ml pepstatin, 1 μg/ml antipain, and 1 mM iodoacetamide) for 20 min on ice. The entire monolayer was released from the culture dish by this procedure. The extracts were collected and centrifuged in an Eppendorf microfuge (Brinkmann Instruments, Inc., Westbury, NY) at full speed for 1 min at room temperature. Extracts were divided into supernatants and pellets. The pellets were solubilized in 100 μl 50 mM Tris, pH 8.8, 5 mM EDTA, 1% (wt/vol) SDS (solubilization buffer), heated 3 min at 95°C, and passed through a 22G needle several times to shear DNA. In preparation for immunoprecipitation, the solubilized pellets were diluted 1:10 with extraction buffer and the Triton-solubilized supernatants were brought to the same concentration of SDS as the pellet fractions by addition of 100 μl solubilization buffer.

PKHA cells were grown on 30 mm Millicell-HA filters (Millipore Corp.) to permit efficient labeling from the basolateral surface. The methionine uptake system in LLC-PK1 cells is concentrated on the basolateral plasma membrane (1, 22, 38). For pulse-labeling, the filters were placed on 0.5 ml Earle's MEM without methionine (Sigma Chemical Co.) supplemented with 15 mM Hepes, pH 7.3, 0.035% sodium bicarbonate (labeling medium), containing 50 μCi [^{35}S]methionine and incubated for 15 min in a waterbath at 37°C. They were then chased in medium containing excess methionine added apically and basolaterally. The cells were extracted by cutting out the filters and placing them in micro-Eppendorf tubes (Brinkmann Instruments, Inc.) containing 1.0 ml extraction buffer and inverting them for 20 min at 4°C. The tubes were centrifuged to push the filters to the bottom and the supernatants removed. Insoluble material still attached to the filter was extracted by adding 100 μl solubilization buffer and heating 3 min at 95°C. The extract was diluted 1:10 with extraction buffer and transferred to a new tube, discarding the filter.

For labeling, MDCK cells in suspension were removed from the spinner flask and washed twice with labeling media (containing 0.22% sodium bicarbonate for labeling in the 5% CO_2 incubator) by centrifugation at 2,000 rpm for 5 min in the tabletop centrifuge. The cells (5×10^6 cells/ml) were pulse-labeled for 5 min with 1 mCi [^{35}S]methionine in 5 ml labeling media and diluted 10-fold with excess methionine medium. At appropriate timepoints, 5-ml samples were removed, immediately diluted in ice cold PBS to stop further transport of labeled material, washed once by centrifugation, and resuspended in 1.0 ml extraction buffer. After inverting 20 min at 4°C, the samples were spun in the microfuge, separated into supernatants and insoluble pellets, and prepared for immunoprecipitation as described above.

Trypsin Assay

To detect cell surface hemagglutinin, cells grown on plastic dishes were treated with trypsin (Sigma Chemical Co.) as previously described (20) except 200 μg/ml soybean trypsin inhibitor was used. PKHA cells on filters were treated as described previously for MDCK cells on filters (21).

MDCK cells from suspension cultures were trypsinized by resuspending them in 5 ml 100 μg/ml trypsin in PBS on ice for 15 min with gentle agitation. The cells were pelleted and resuspended in 5 ml 200 μg/ml soybean trypsin inhibitor in PBS for 10 min on ice, and extracted with 1.0 ml extraction buffer for 20 min at 4°C.

1. *Abbreviations used in this paper*: CEF, chick embryo fibroblast; dMM, deoxymannojirimycin.

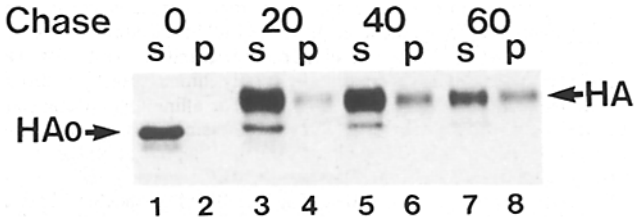

Figure 1. Appearance of hemagglutinin in the insoluble fraction of MDCK cell extracts. Infected MDCK cells were pulse-labeled for 5 min with 50 μCi [^{35}S]methionine at 37°C and then incubated with excess unlabeled methionine for various times. The cells were extracted with 1% Triton X-100 extraction buffer at 0°C and the extract separated by centrifugation into Triton-soluble supernatants (*s*) and -insoluble pellets (*p*). Hemagglutinin was immunoprecipitated with affinity-purified polyclonal antiserum and analyzed by SDS gel electrophoresis and fluorography. HAo is the form of hemagglutinin with core oligosaccharides seen just after the pulse-label. After chase incubations, hemagglutinin migrates more slowly due to the addition of complex oligosaccharides (*HA*, lanes *3–8*). Insoluble hemagglutinin is first observed at 20-min chase (lane *4*) and at all subsequent timepoints (lanes *6* and *8*). Only the HA form of hemagglutinin is insoluble in Triton. The faint band of HAo observed in lane *2* is <2% of the total radioactivity in hemagglutinin.

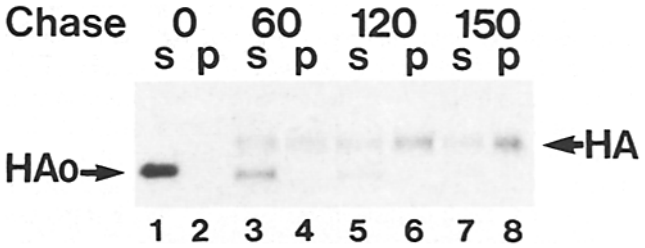

Figure 2. Hemagglutinin insolubility is not dependent on a viral infection. PKHA cells, transfected with a cDNA for hemagglutinin, were pulse-labeled 10 min with 50 μCi [^{35}S]methionine and chased as described in Materials and Methods. The cells were extracted with 1% Triton X-100 extraction buffer and the extract separated by centrifugation into supernatants (*s*) and pellets (*p*). Hemagglutinin was immunoprecipitated with a polyclonal antiserum and analyzed by SDS gel electrophoresis and fluorography. Insoluble hemagglutinin is first evident at 60 min (lane *4*) and at all subsequent times throughout the chase incubation (lanes *6* and *8*). As with infected MDCK cells, only the HA form of hemagglutinin is insoluble. Although the insoluble form appears more slowly than in MDCK cells, the relative timing is very similar (see Results).

Immunoprecipitation

The hemagglutinin from Triton-soluble supernatants and -insoluble pellets solubilized in SDS was immunoprecipitated overnight at 4°C with saturating amounts of H28-E23 culture supernatant, affinity-purified H28-E23, or affinity-purified rabbit polyclonal antiserum. Protein A–Sepharose (25 μl of a 1:1 slurry) (Pharmacia Inc.) or 25 μl protein A-Trisacryl (1:1 slurry) (Pierce Chemical Co.) was added and samples inverted for 2 h at 4°C. The immunoprecipitates were washed three times with 10 mM Tris, pH 8.6, 0.5 M NaCl, 1% (wt/vol) Triton X-100, 0.1% (wt/vol) SDS (wash buffer), and once with 10 mM Tris, pH 8.6. Immunoprecipitates were resuspended in 15 μl 50 mM Tris, pH 8.8, 5 mM EDTA, 10% (wt/vol) sucrose, 0.1% (wt/vol) bromophenol blue (gel sample buffer), 1% (wt/vol) SDS, reduced by addition of 5 μl 0.2 M DTT, and heated for 3 min at 95°C. Samples were alkylated by addition of 5 μl 0.5 M iodoacetamide, incubated at 37°C for ~15 min, and separated on a 7.5–15% polyacrylamide gradient gel in a Tris-glycine buffer system (20, 37).

Quantitation

The amount of hemagglutinin in Triton-soluble and -insoluble fractions was quantitated by cutting out bands from dried gels, as previously described (20, 60). The results are reported as the percentage of the total radioactivity in hemagglutinin derived from a single plate of cells, including both soluble supernatant and insoluble pellet. Because HA2 was lost from immunoprecipitates of some fractions, it was assumed for quantitation that the amount of radioactivity in HA2 was twice that of HA1 in the immunoprecipitate. This assumption was valid because there are twice the number of methionines in HA2 as in HA1 in PR8 hemagglutinin (62).

Inhibition of Complex Oligosaccharide Addition

To block addition of complex oligosaccharides, infected MDCK cells were preincubated 15 min with 1 mM deoxymannojirimycin (dMM) (Boehringer Mannheim Biochemicals, Indianapolis, IN) in labeling medium. The cells were then pulse-labeled and chased in the presence of 1 mM dMM as previously described (5).

Immunofluorescence

MDCK cells were cultured on glass coverslips to subconfluency and infected with ts61S for 6 h at 39°C. Some cells were then incubated at 20°C for 2 h while others were incubated at 20°C for 2 h and then switched to 33°C for an additional 15–30 min. All of the incubations after the initial 6-h infection were performed in the presence of 20 μg/ml cycloheximide to block further protein synthesis. After incubation at the various temperatures, cells were placed on ice and either fixed with methanol at −20°C for 5 min, or extracted for 10–30 s with extraction buffer and then fixed. Longer extractions caused the cell to come off the coverslips. Nonspecific binding of antibodies was prevented by incubation of the coverslips with PBS/0.2% (wt/vol) gelatin before staining by the indirect technique. The first antibody was the H15-E8 culture supernatant and the second antibody was 1:100 dilution of goat anti-mouse immunoglobulins conjugated to rhodamine (Tago Inc., Burlingame, CA).

Because the length of extraction used for the immunofluorescence experiment was much shorter than that used in the pulse-chase experiments, a control was performed to be certain that the results were comparable. MDCK cells infected with PR8 influenza were pulse-labeled, chased, and then extracted for the same amount of time as the coverslips. The supernatants from the control plates were collected and immunoprecipitated. The material remaining on the plates was fixed with methanol, extracted with 100 μl SDS containing solubilization buffer, diluted 1:10 with extraction buffer, and immunoprecipitated.

Trypsinization of Hemagglutinin in Permeabilized Cells

To cleave both intracellular and cell surface hemagglutinin with trypsin, infected MDCK cells were pulse-labeled, chased, and divided into two groups. The first group was treated with trypsin without permeabilization as already described. The second group was permeabilized and trypsinized by addition of 100 μl 0.5% (wt/vol) Triton X-100, 0.1 mg/ml trypsin, and 40 mM *N*-ethylmaleimide in PBS on ice for 15 min. To block the trypsin, soybean trypsin inhibitor (10 μl of a 1.0 mg/ml solution in PBS) was added for 10 min. The cells were solubilized by addition of 100 μl 50 mM Tris, pH 8.8, 5 mM EDTA, 4% (wt/vol) SDS. Nonpermeabilized cells were solubilized with the same buffer after the addition of 110 μl PBS. The plates were scraped in the SDS solution with a bent 22G needle, the extract sheared, and heated at 95°C for 3 min to denature the hemagglutinin. A 50-μl aliquot of each sample was diluted with 1.0 ml extraction buffer and immunoprecipitated. The samples were separated by SDS gel electrophoresis and the bands detected by fluorography. The radioactive bands were cut out of the gels and incorporation was measured as described above.

Results

Hemagglutinin Becomes Detergent Insoluble During Transport

MDCK cells infected with influenza virus synthesize pre-

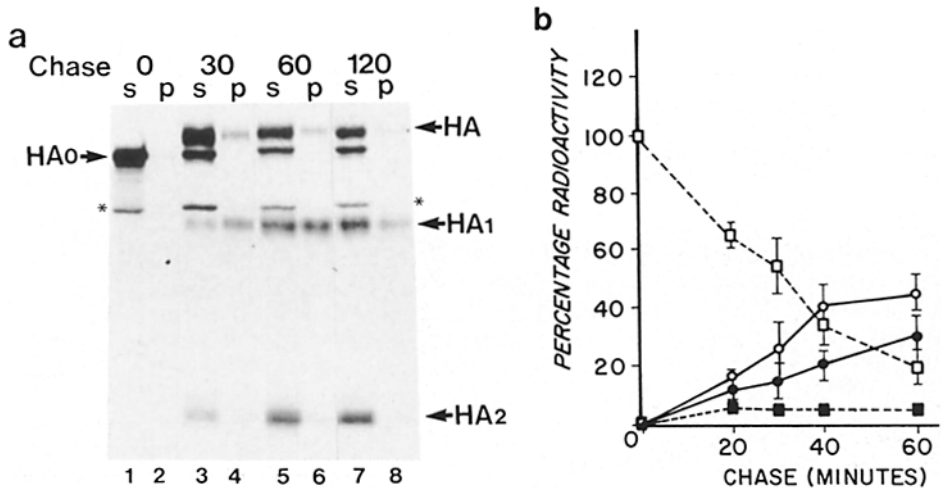

Figure 3. Insolubility is first detected in hemagglutinin that has not yet reached the plasma membrane. Infected MDCK cells were pulse-labeled and chased as described in the legend to Fig. 1. The cells were trypsinized at 0°C to cleave hemagglutinin on the plasma membrane and extracted with Triton. The extracts were separated by centrifugation into soluble supernatants (*s*) and insoluble pellets (*p*). Hemagglutinin was immunoprecipitated and analyzed by SDS gel electrophoresis and fluorography. In *a*, a fluorograph of an SDS gel from a typical experiment is shown; in *b*, the quantitative results of 3–11 experiments, obtained by cutting out and counting bands from dried gels, are displayed graphically. The error bars refer to the standard deviations. Absence of error bars indicates that the standard deviations were too small to depict. Hemagglutinin is first detected on the cell surface at ~20–30-min chase, as indicated by the appearance of the trypsin cleavage products HA1 and HA2 (*a*, lanes *3–8*). During the chase incubation, the amount of soluble, uncleaved hemagglutinin declines (*a*, *HA* in lanes *3*, *5*, and *7*; *b*, □) while the amounts of soluble cleavage products increases (*a*, *HA1* and *HA2* in lanes *3*, *5*, and *7*; *b*, ○). In the insoluble pellets, the amount of uncleaved hemagglutinin remains constant during the chase (*a*, *HA* in lanes *4*, *6*, and *8*; *b*, ■) while the amount of cleaved hemagglutinin increases (*a*, *HA1* in lanes *4*, *6*, and *8*; *b*, ●). The presence of uncleaved hemagglutinin in the insoluble fraction indicates that insolubility commences before hemagglutinin reached the cell surface. The HA2 band.is almost completely absent from the insoluble fractions (*a*, lanes *4*, *6*, and *8*). Because of this, the amount of radioactivity in cleaved hemagglutinin was calculated by tripling the counts per minute measured in HA1 (see Materials and Methods for additional details). The band marked with an asterisk is the viral capsid protein NP that contaminates the immunoprecipitates.

dominantly viral proteins (20, 21, 23). Hemagglutinin synthesis, transport, and processing can be analyzed by pulse-labeling the cells and after subsequent chase incubations, examining changes in hemagglutinin mobility using SDS gel electrophoresis. The pulse-labeled hemagglutinin band migrates with an apparent molecular mass of 68,000 D (*HAo*, Fig. 1, lane *1*). After 20-min incubation in chase medium, hemagglutinin migrates slower than just after the pulse-label (*HA*, Fig. 1, lane *3*). The mobility shift corresponds to the addition of complex oligosaccharides (20). The half-time for the conversion from HAo to HA is ~20 min (20).

When influenza virus–infected MDCK cells were pulse-labeled, chased, and extracted with Triton X-100 under isotonic conditions at pH 7.4, and the extract immunoprecipitated with a monoclonal antibody, there appeared to be a progressive loss of hemagglutinin from the extract with longer chase incubations. In an attempt to recover the missing hemagglutinin, the Triton-insoluble pellets normally discarded after extraction were examined. At early times after the pulse-label, no hemagglutinin was detected in the pellet when it was solubilized in SDS and immunoprecipitated (Fig. 1, lane *2*). Hemagglutinin was, however, found in the pellet beginning at ~15–20-min chase (Fig. 1, lane *4*). The amount of hemagglutinin in the pellet increased with longer chase times to a maximum of 26% of the total radioactivity in hemagglutinin at 60 min.

The amount of hemagglutinin resistant to detergent extraction was not dependent on the batch of detergent used to extract the cells or the detergent to protein ratio. Insoluble hemagglutinin was found when highly purified Triton X-100 (low in peroxide and carbonyl content) was used or when NP-40 was substituted. Doubling the volume of the extraction buffer also had no effect on the appearance of hemagglutinin in the insoluble fraction.

Hemagglutinin did not seem to be stably associated with the insoluble pellet since reextraction with Triton X-100 released additional hemagglutinin (data not shown). However, hemagglutinin was not simply trapped in the pellet because at early chase times it was never found in the pellet in amounts >1–3% of the total radioactivity. In addition, mixing of soluble supernatants from infected cells with pellets from uninfected cells did not cause hemagglutinin to partition into the pellet. Hemagglutinin insolubility was also not due to intermolecular disulfide crosslinks because including DTT in the extraction buffer did not alter the amount of extractable hemagglutinin.

Since only mature hemagglutinin was insoluble, it was possible that complex oligosaccharides were contributing to the insolubility. To address this, dMM was used to block the modification of oligosaccharides to the complex form. dMM prevents trimming of mannose residues by inhibiting mannosidase I (8), but it does not alter the rate of hemagglutinin transport or the amount transported to the plasma membrane (5). Despite inhibition of trimming by dMM, the appearance of insoluble hemagglutinin was not effected (not shown).

In summary, these experiments demonstrated that hemagglutinin became resistant to extraction after the acquisition of complex sugars, late in the transport pathway to the apical plasma membrane. Complex sugars were, however, not required for hemagglutinin to become Triton insoluble.

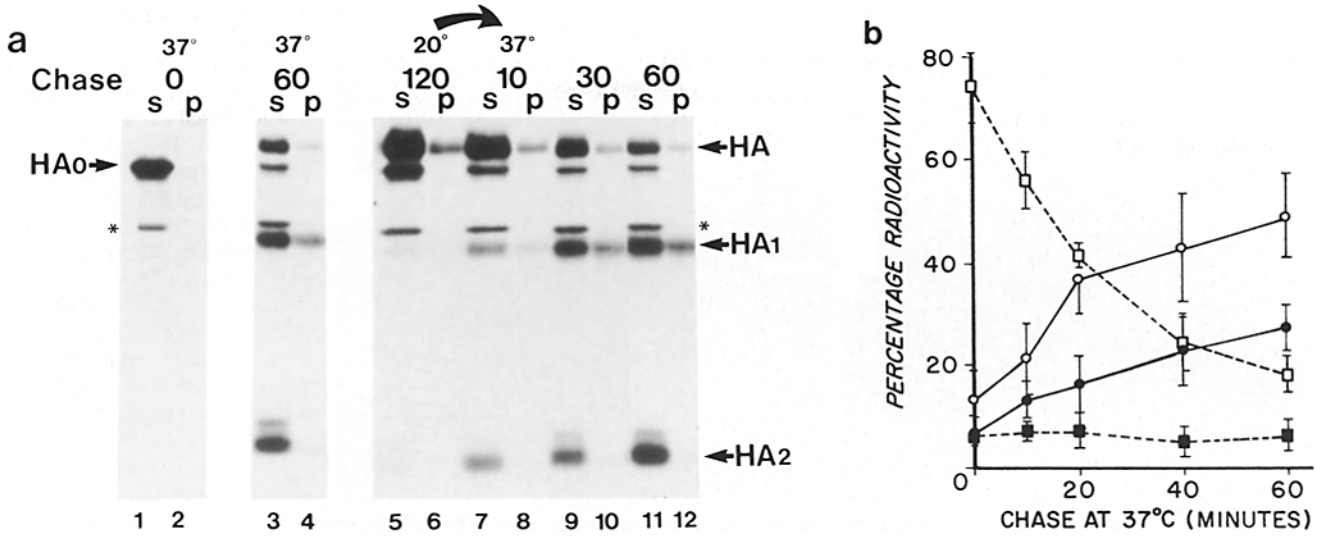

Figure 4. Insoluble hemagglutinin is detected when transport to the plasma membrane is blocked. Infected MDCK cells were pulse-labeled 5 min with [^{35}S]methionine at 37°C and then transferred to chase medium at 19–20°C for 2 h. The temperature block was released by transferring the cells back to 37°C chase medium. The cells were trypsinized and extracted, and hemagglutinin immunoprecipitated with affinity-purified polyclonal antiserum. In *a*, a fluorograph of an SDS gel from a typical experiment is shown; in *b*, quantitative results from three experiments are illustrated graphically. The error bars refer to the standard deviations. Lanes *1–4* of *a* illustrate the distribution of hemagglutinin in soluble and insoluble fractions just after the pulse label (*a*, lanes *1* and *2*) and after a 60-min chase at 37°C (*a*, lanes *3* and *4*). After 2 h at 20°C, almost all hemagglutinin is uncleaved and therefore intracellular (*a*, lanes *5* and *6*; *b*, 0 time, □ and ■). Most hemagglutinin at this time is soluble (*a*, lanes *5*; *b*, 0 time, □). A small amount of hemagglutinin at this time is insoluble (*a*, lane *6*; *b*, ■). Upon warming at 37°C, the amount of soluble uncleaved hemagglutinin declines (*a*, lanes *7*, *9*, and *11*; *b*, □), while the amount of insoluble uncleaved hemagglutinin remains constant (*a*, lanes *8*, *10*, and *12*; *b*, ■). Both soluble and insoluble hemagglutinin increase in amount (*a*, lanes *7–12*; *b*, ○ and ●). As before, HA2 is lost from the insoluble fractions (*a*, lanes *8*, *10*, and *12*). The asterisk refers to the capsid protein NP contaminating the immunoprecipitates.

Appearance of Insoluble Hemagglutinin Does Not Depend on a Viral Infection

Since insoluble hemagglutinin appeared late in transport it was possible that insolubility was due to the interaction of hemagglutinin with other viral proteins during virus budding. To address this concern, hemagglutinin solubility was investigated in LLC-PK1 cells stably transfected with the cDNA for hemagglutinin of the H2 subtype (PKHA cells).

PKHA cells were pulse-labeled with [^{35}S]methionine for 15 min, chased, extracted, and immunoprecipitated (Fig. 2). As in infected MDCK cells, hemagglutinin was completely soluble just after the pulse-label and at early chase times. Insoluble hemagglutinin appeared at 60-min chase, after the addition of complex sugars (Fig. 2, lane *4*). Although the appearance of insoluble hemagglutinin commenced later than in infected MDCK cells, the relative timing of appearance was identical because processing and intracellular transport of hemagglutinin to the plasma membrane occurs more slowly in PKHA cells (48; unpublished results). The amount of insoluble hemagglutinin was higher than the amount measured in infected MDCK cells, reaching ~45% of the total radioactivity in hemagglutinin at 120-min chase (Fig. 2, lanes *5* and *6*).

On the basis of these experiments, it was clear that hemagglutinin insolubility was unrelated to virus budding, the viral infection, or other viral components. In addition, these results demonstrated that hemagglutinin insolubility was not restricted to a particular viral subtype or cell line.

Hemagglutinin Becomes Insoluble Before Reaching the Plasma Membrane

The results in MDCK cells indicated that hemagglutinin first became insoluble at ~15–20 min after pulse-labeling, after the addition of complex sugars. To determine where in the cell insolubility commenced, the relationship of insolubility to plasma membrane appearance was examined. Native hemagglutinin possesses a single trypsin sensitive site that is efficiently cleaved at 0°C (17, 19, 20). Digestion with trypsin can therefore be used to quantitate hemagglutinin on the plasma membrane (20). The two polypeptides resulting from trypsin cleavage remain associated by a single disulfide bond and other noncovalent interactions between the polypeptide chains. Upon reduction and denaturation the polypeptides migrate as two bands on SDS gels of 50,000 (*HA1*) and 27,000 D (*HA2*, see Fig. 3 *a*, lane *5*).

When pulse-labeled MDCK cells were trypsinized and extracted, both the soluble and insoluble fractions contained uncleaved hemagglutinin (*HA*) and the fragments HA1 and HA2 after 30-min chase (Fig. 3 *a*). As the amount of soluble cleaved hemagglutinin increased at longer chase times, in-

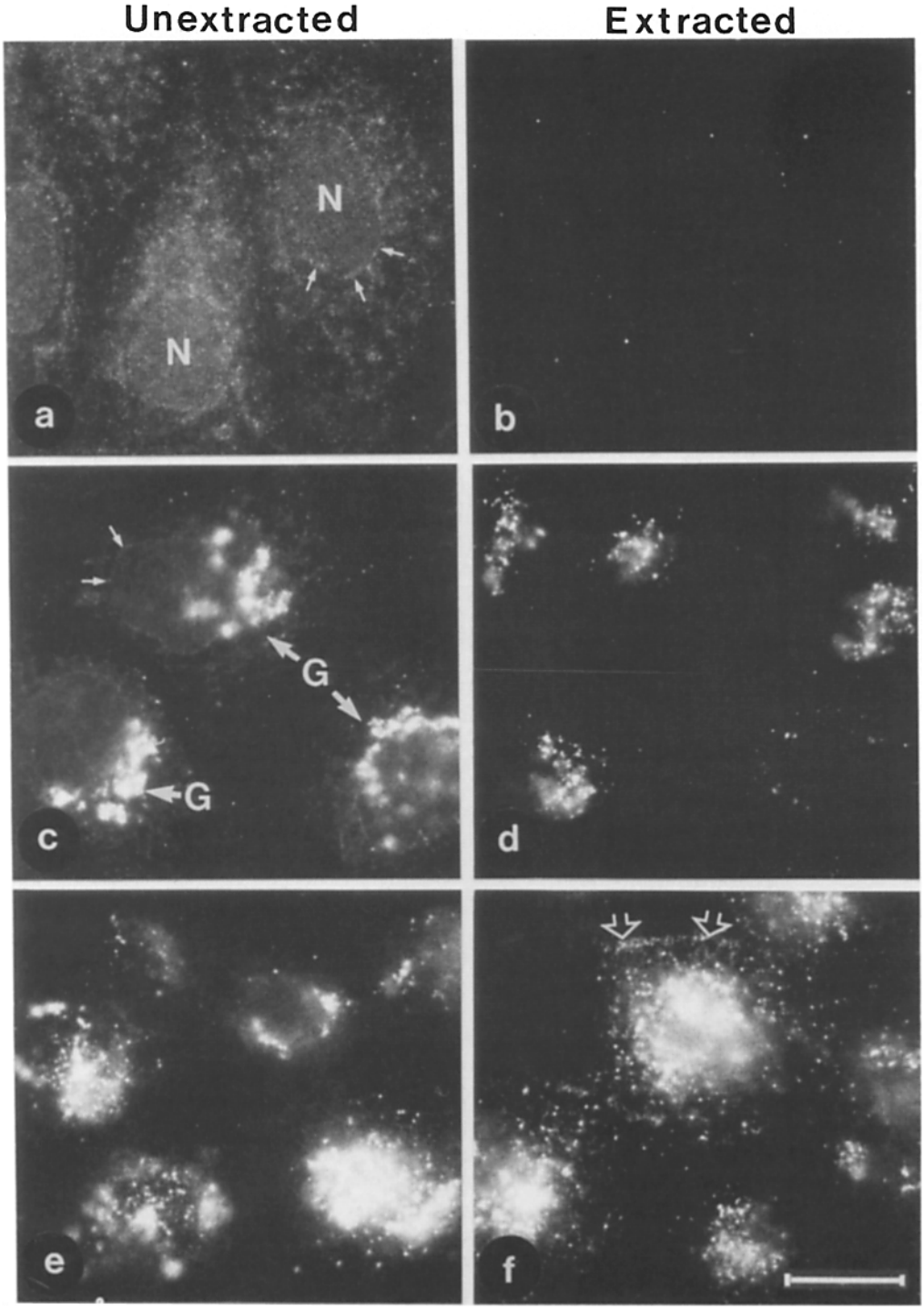

Figure 5. Localization of insoluble hemagglutinin by immunofluorescence. MDCK cells grown on glass coverslips were infected with ts61S and incubated at the nonpermissive temperature, 39°C, for 6 h (*a* and *b*). Some cultures were then transferred to 20°C for 2 h in the presence of 20 μg/ml cycloheximide (*c* and *d*). A third set of coverslips was transferred to the permissive temperature of 33°C for 15 min, after 2 h at 20°C (*e* and *f*). Cells from each set were fixed directly in −20°C methanol (*a*, *c*, and *e*) or were extracted for 30 s with 1% Triton X-100 extraction buffer before fixation (*b*, *d*, and *f*). *N*, nucleus, *G*, Golgi complex. (*Small arrows*) Nuclear membrane; (*large open arrows*) plasma membrane. Bar, 10 μm.

soluble cleaved hemagglutinin also increased (Fig. 3 *b*, *open* and *solid circles*). Concomitantly, there was a striking loss of HA2 in the insoluble pellet (Fig. 3 *a*, lanes *4*, *6*, and *8*; see below).

The amount of insoluble hemagglutinin not cleaved by trypsin reached a plateau of ~5% of the total label (Fig. 3 *b*, *solid squares*). This small amount of uncleaved hemagglutinin was not due to inefficient cleavage of protein on the plasma membrane by trypsin because the amount of cleaved insoluble hemagglutinin continued to increase with longer chase incubations. Inefficient cleavage would produce a constant ratio of cleaved to uncleaved hemagglutinin; in fact, the ratio of intracellular insoluble hemagglutinin to cleaved insoluble hemagglutinin decreased with continued incubation (Fig. 3 *b*, *solid circles* and *squares*).

To further substantiate these findings, the appearance of insoluble hemagglutinin was examined when transport to the plasma membrane was reversibly blocked in the *trans*-Golgi by incubating the cells at 19–20°C (Fig. 4 *a*) (20). MDCK cells were pulse-labeled at 37°C and then chased for 2 h at

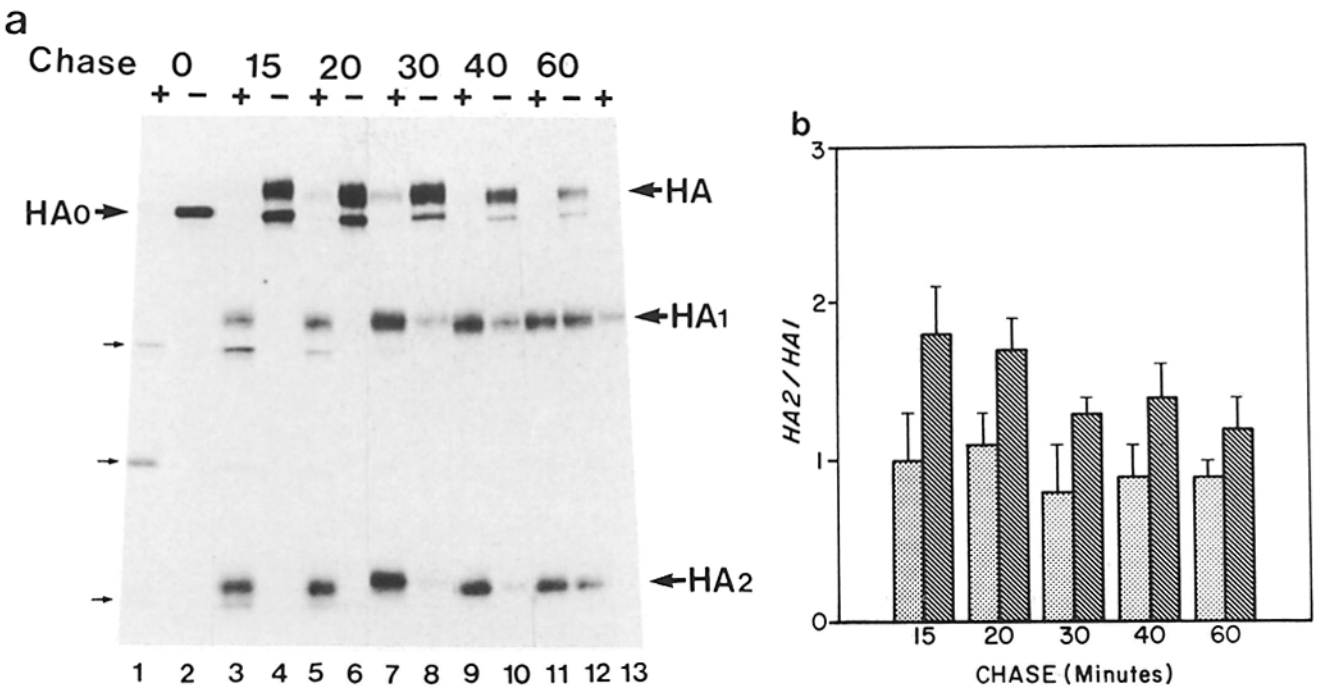

Figure 6. Loss of the disulfide bond linking HA1 and HA2 during intracellular transport. Infected MDCK cells were pulse-labeled and chased as described in the legend to Fig. 1. Cells were placed on ice and either trypsinized at the cell surface or in the presence of 0.5% Triton X-100 to permeabilize the cells. Hemagglutinin was extracted and denatured with SDS at 95°C, immunoprecipitated with anti-HA1 antibodies, and analyzed by SDS gel electrophoresis and fluorography. In *a*, a fluorograph from a typical experiment is shown. Lanes marked + indicate trypsinization after permeabilization with Triton; lanes marked with − indicate trypsinization in the absence of permeabilization from the cell surface. At time 0, trypsinization of hemagglutinin after permeabilization cuts the protein into multiple bands (*arrows*, lane *1*) because trimerization of the molecule has not yet occurred. At later times, almost all of the hemagglutinin is cut into HA1 and HA2 by trypsinization of permeabilized cells (lanes *3*, *5*, *7*, *9*, and *11*). As a control, one sample was treated with DTT after trypsinization to chemically reduce the disulfide bond between HA1 and HA2; under these conditions, all of HA2 is lost from the immunoprecipitate (lane *13*). In *b*, the quantitative results of three experiments are tabulated. Absence of the disulfide bond is assayed by the loss of HA2 from immunoprecipitates resulting in a decline in the ratio of radioactivity in HA2 to that in HA1. If HA2 is quantitatively recovered (that is, if the disulfide bond is intact) then the ratio should be 2:1. As shown here, the ratio declines in samples treated with trypsin after permeabilization (*hatched bars*) to a level of ~1. In cells treated with trypsin at the cell surface, the ratio is ~1 at all times (*stippled bars*), suggesting that the disulfide bond linking HA1 and HA2 is absent in about half of the hemagglutinin molecules. See Results and Materials and Methods for further details. Error bars, SD.

19–20°C. Under these conditions most hemagglutinin was uncleaved and soluble in Triton X-100 (Fig. 4 *a*, lane *5*). Some insoluble uncleaved hemagglutinin was also observed (Fig. 4 *a*, lane *6*). When the temperature was shifted from 19–20 to 37°C, cleaved and uncleaved hemagglutinin were seen in both the soluble and insoluble fractions (Fig. 4 *a*, lanes *7–12*). With continued incubation, the cleaved insoluble fraction increased while the uncleaved insoluble fraction remained constant (Fig. 4 *b*, *solid circles* and *squares*). At the same time, cleaved soluble hemagglutinin increased while uncleaved soluble hemagglutinin declined (Fig. 4 *b*, *open circles* and *squares*).

On the basis of both the experiments at 37 and 20°C, it seemed clear that changes in hemagglutinin leading to insolubility commenced inside the cell, possibly as soon as the *trans*-Golgi, and that they persisted after transport to the plasma membrane.

Insoluble Hemagglutinin Can Be Localized to the Golgi and Plasma Membrane by Immunofluorescence

Because sorting of apical proteins from basolateral proteins in MDCK cells occurs during transport from the Golgi complex to the plasma membrane, and because hemagglutinin insolubility appeared to commence intracellularly late on the transport pathway, it was of interest to examine hemagglutinin insolubility morphologically. To visualize insoluble hemagglutinin in MDCK cells, infected cells were extracted with Triton X-100 and examined by immunofluorescence. MDCK cells were infected with the ts61S temperature-sensitive mutant of influenza at the nonpermissive temperature of 39°C for 6 h. At this temperature, transport of hemagglutinin is blocked in the endoplasmic reticulum (40). In cells transferred to 20°C for 2 h in the presence of cycloheximide, the hemagglutinin synthesized at 39°C is transported to the *trans*-Golgi but does not reach the cell surface (40). If the cells are then incubated at the permissive temperature of 33°C, hemagglutinin is transported from the *trans*-Golgi to the plasma membrane (40).

After infection at the nonpermissive temperature, staining for hemagglutinin was diffuse throughout the cytoplasm and slightly enhanced around the nucleus, characteristic of the endoplasmic reticulum (Fig. 5 *a*). Extraction before fixation

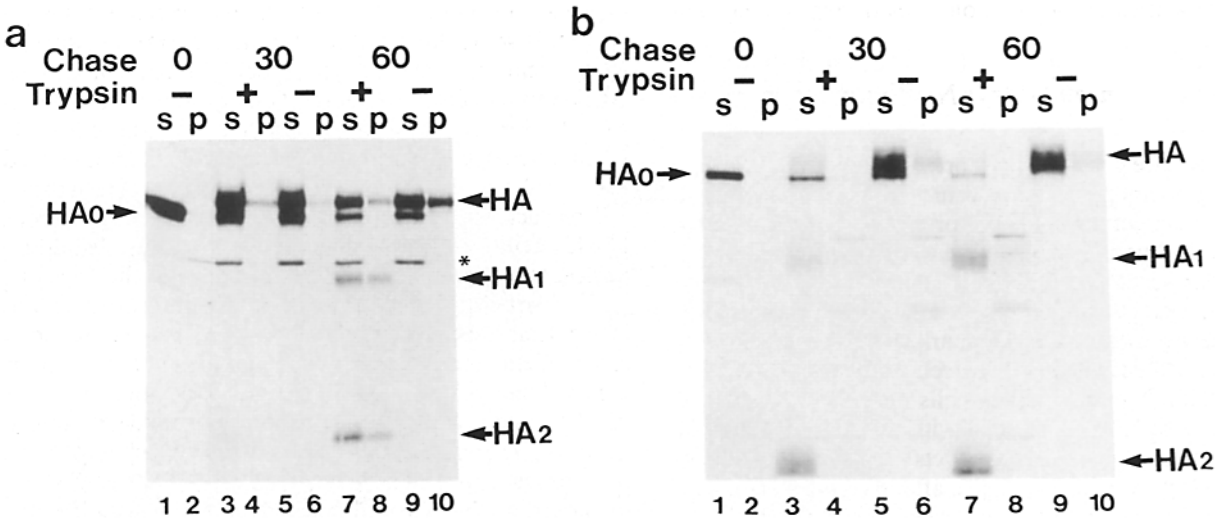

Figure 7. Insoluble hemagglutinin is also detected in depolarized and unpolar cells. (*a*) MDCK cells cultured in suspension were infected, pulse-labeled, and chased. Some samples were treated with trypsin to cleave cell surface hemagglutinin (+) and some were not (−). Cells were extracted with Triton and hemagglutinin immunoprecipitated from the soluble (*s*) and insoluble (*p*) fractions. Insoluble hemagglutinin was detected beginning at 30-min chase (lanes *3–10*). The asterisk indicates the capsid protein NP contaminating the immunoprecipitates. (*b*) Infected CEF cells were pulse-labeled, chased, trypsinized, and extracted. The extracts were centrifuged and hemagglutinin immunoprecipitated from supernatants (*s*) and pellets (*p*). Insoluble hemagglutinin was detected beginning at 30-min chase (lanes *3–10*). The amount of insoluble hemagglutinin was less than that seen in MDCK cells (see *a* and Fig. 4). Since hemagglutinin made by the fibroblasts migrates diffusely on gels, insoluble material is barely visible in samples treated with trypsin (lanes *4* and *8*).

eliminated this staining almost completely (Fig. 5 *b*). The cells incubated at 20°C exhibited a perinuclear staining resembling that of the Golgi complex (Fig. 5 *c*). Upon extraction of a parallel sample, a punctate staining still localized to the Golgi region was evident (Fig. 5 *d*). When cells were incubated for 15 min at the permissive temperature, both residual Golgi complex and cell surface staining were observed. When cultures incubated in this way were extracted, little difference between extracted and unextracted was noted (Fig. 5, *e* and *f*).

The observations by immunofluorescence confirmed and extended the previous findings using the biochemical approach. Hemagglutinin was completely Triton soluble early in the transport pathway. When blocked in the *trans*-Golgi, a small amount of hemagglutinin was insoluble. Finally, by the time the protein reached the plasma membrane, a much larger fraction had become resistant to extraction.

Disulfide Bond Connecting HA1 and HA2 Is Reduced in Insoluble Hemagglutinin

As noted earlier, in immunoprecipitates of trypsin-cleaved hemagglutinin from the insoluble pellet, the amount of HA2 was diminished relative to the expected HA2 to HA1 ratio (Fig. 3 *a*). Theoretically, separation of hemagglutinin into the HA1 and HA2 subunits requires three steps. First hemagglutinin must be cut with trypsin; second, the disulfide bond linking HA1 and HA2 must be reduced; third, hemagglutinin must be denatured to break interactions between polypeptide chains. In the experiment shown in Fig. 3 *a*, hemagglutinin had been digested with trypsin, denatured by treatment with SDS, and then immunoprecipitated with an HA1-specific antibody. Under these conditions, HA2 should have been quantitatively recovered in the immunoprecipitates if the disulfide bond between HA1 and HA2 was intact. Instead, HA2 was lost, suggesting that the disulfide bond was absent (Fig. 3 *a*).

Because the loss of HA2 could only be detected in hemagglutinin cleaved with trypsin, and because trypsin only had access to the cell surface in the experiment shown in Fig. 3 *a*, it was not clear if the disulfide bond was absent as well in intracellular hemagglutinin. To examine this, pulse-labeled MDCK cells were permeabilized with low concentrations of Triton X-100 in the presence of trypsin and *N*-ethylmaleimide to cleave both intracellular and cell surface hemagglutinin. *N*-ethylmaleimide was included to react with any free sulfhydryls and block formation of artifactual disulfide bonds. In parallel samples, pulse-labeled MDCK cells were trypsinized at the cell surface without permeabilization. The samples were solubilized in SDS with heating to denature hemagglutinin, immunoprecipitated with HA1 specific antibodies, and analyzed by SDS gel electrophoresis (Fig. 6 *a*). If the disulfide bond of the denatured hemagglutinin was intact at the time of immunoprecipitation, the ratio of radioactivity in HA2 to HA1 should approximate the ratio of methionines, 2:1. If the ratio was less than this, then it would suggest that the disulfide was broken before immunoprecipitation.

At early chase times the ratio of HA2/HA1 was near the theoretical 2:1 ratio indicating that the disulfide bond was initially formed (Fig. 6 *b*, *15 min*, *hatched bar*). This ratio fell at later times reflecting a dramatic loss of HA2 (Fig. 6 *b*, *60 min*, *hatched bar*). The ratio of HA2/HA1 for hemagglutinin cleaved at the cell surface approximated 1:1 at all chase times (Fig. 6 *b*, *stippled bars*). In control samples artificially reduced with DTT all HA2 was absent after immunoprecipitation with HA1-specific antibodies indicating that the denaturation conditions were sufficient to fully separate HA1 and HA2 after reduction of the connecting disulfide bond (Fig. 6 *a*, lane *13*).

In summary, the disulfide bond linking HA1 and HA2 is formed at the time of hemagglutinin synthesis but is broken

in at least a fraction of the molecules during intracellular transport.

Hemagglutinin Insolubility Is Not Restricted to Polarized Cells

MDCK cells are polarized and sort hemagglutinin to the apical plasma membrane. To determine if the presence of insoluble hemagglutinin could be correlated with cell polarity, the extractability of hemagglutinin was examined in depolarized MDCK cells and CEF.

MDCK cells were cultured as a single cell suspension. Under these conditions, apical markers have been shown to be randomly distributed over the cell surface (44). After infection with influenza virus, the cells were pulse-labeled and chased in suspension, extracted with Triton X-100, and the soluble extracts and insoluble pellets analyzed. As with polarized cells grown on plastic, just after the pulse-label, little insoluble hemagglutinin was observed (Fig. 7 *a*, lane *2*). Insoluble hemagglutinin was detectable at 30-min chase, after the acquisition of complex oligosaccharides (Fig. 7 *a*, lane *4*), and at 60 min, the amount of insoluble hemagglutinin was similar to that seen in MDCK cells grown on plastic (Fig. 7 *a*, lane *10*).

Insoluble hemagglutinin was also observed in CEF that are known to express hemagglutinin over the entire cell surface (43). Primary cultures of CEF were infected with influenza virus, pulse-labeled, chased, and extracted identically to MDCK cells. As with polarized MDCK cells, insoluble hemagglutinin appeared in a transport-dependent manner (Fig. 7 *b*). Cell surface appearance and onset of hemagglutinin insolubility was slowed in these cells, but the timing of insolubility relative to complex sugar addition and cell surface appearance was similar to that seen in MDCK cells (Fig. 7 *b*, lanes *3–10*). The hemagglutinin bands on the polyacrylamide gel from CEF cells were diffuse and the amount of hemagglutinin in the insoluble fraction appeared less than in MDCK cells.

Discussion

Differential Solubility of Hemagglutinin During Intracellular Transport

The experiments described here establish that the influenza virus hemagglutinin becomes resistant to extraction with isotonic solutions of Triton X-100 late in transport to the apical plasma membrane in infected MDCK cells. At early times, it is completely soluble under identical extraction conditions.

After 60-min chase, insoluble hemagglutinin amounted to ~26% of that labeled by a 5-min pulse. Because solubilization of the detergent-resistant pellet required denaturation of the hemagglutinin, immunoprecipitation of the insoluble material was inefficient. Trichloroacetic acid precipitates of the residues left after immunoprecipitation always contained additional hemagglutinin. This problem was not corrected by increasing the amount of monoclonal antibody or by using a polyclonal antiserum for immunoprecipitation. By comparison, ~45% of the hemagglutinin made by the transfected PKHA cells was insoluble under identical conditions. The quantitative discrepancy between the two situations can be explained by either differences in hemagglutinin subtype structures which limit the denaturation in SDS solutions, or by the ability of the subtype specific antiserum to more efficiently recognize denatured hemagglutinin from PKHA cells. It is clear, nevertheless, that the estimate of 26% insoluble hemagglutinin in the infected cells is an underestimate, and that the actual amount could be much higher.

The fact that hemagglutinin produced by transfected PKHA cells was also differentially insoluble definitively demonstrated that insolubility was not due to the formation of viral particles late in transport, or to some other side effect of the viral infection. Insolubility occurs as a consequence of the interaction between hemagglutinin and the transporting machinery of the cell and not from association with other virally encoded components. In this sense, hemagglutinin insolubility resembles other aspects of hemagglutinin transport, processing, and sorting, all of which have been shown to depend on the host cell rather than on the viral infection (46, 52).

Even though most insoluble hemagglutinin was on the cell surface, insolubility commenced intracellularly. Approximately 5% of the total pulse-labeled hemagglutinin was insoluble and resistant to trypsin added to the cell surface. The failure of this small fraction of the insoluble hemagglutinin to be cleaved by trypsin indicated that it was inside the cell. When hemagglutinin transport was arrested in the *trans*-Golgi by incubation at 19–20°C, most pulse-labeled hemagglutinin was soluble. About 5% was insoluble, corresponding exactly to the amount of intracellular insoluble material measured in cells incubated at 37°C. By immunofluorescence as well, a small fraction of the Golgi-associated hemagglutinin was insoluble.

Although hemagglutinin insolubility commences inside the cell, it persists later in transport such that most insoluble hemagglutinin is on the cell surface. It is possible that the level of cell surface insoluble hemagglutinin detected in pulse-chase experiments is maintained by continual addition of insoluble material from the intracellular pool. Preliminary experiments suggest, however, that even under steady state conditions large amounts of insoluble hemagglutinin remain. Alternatively, if hemagglutinin insolubility is caused by binding of hemagglutinin to other proteins, then cell surface hemagglutinin might exist in an equilibrium between free (soluble) and bound (insoluble) forms. The precise size of each pool would depend on dissociation constants and number of available binding sites. In the red cell, for example, the amount of band 3 exceeds that of ankyrin. The result is a relatively large percentage of detergent-soluble band 3 (3, 49).

Other proteins have been previously shown to be insoluble in Triton X-100 under isotonic conditions. Both the erythrocyte anion transporter band 3 and the Na^+/K^+-ATPase in MDCK cells are partially insoluble in Triton solutions (3, 27, 63). Each of these proteins associates with the submembranous spectrin (or fodrin, in MDCK cells) network, probably by means of a primary interaction with ankyrin (28–30, 49). In these cases, therefore, it is likely that insolubility is due to attachment to the cytoskeleton.

Like band 3 and the Na^+/K^+-ATPase, hemagglutinin insolubility may be caused by association with the cytoskeleton. It is unlikely, however, that hemagglutinin interacts with fodrin; in polarized epithelial cells fodrin is found mainly on

the basolateral surface while hemagglutinin is localized to the apical domain (28, 29). It is also conceivable that hemagglutinin associates with microtubules. While the distribution of microtubules in epithelial cells is not completely understood, it is known that microtubule organization is linked to the *trans*-part of the Golgi complex and the centrosome, both of which are present apically in epithelial cells (4, 31, 41). In addition, Rindler et al. reported that drugs affecting microtubule polymerization interfere with the correct sorting of hemagglutinin in MDCK cells, a result contradicted by the findings of Salas et al. (41, 47). Because microtubules would not be expected to remain polymerized when cells are extracted in the cold, as was done here, their involvement in hemagglutinin insolubility seems unlikely.

As an alternative to association with the cytoskeleton, it is possible that insolubility results from coprecipitation of hemagglutinin with other molecules enriched in the distal parts of the transport pathway. Polarized epithelial cells sort not only proteins but lipids to the apical and basolateral cell surfaces (50, 57–59). The apical plasma membrane is enriched in glycolipids, all of which are in the exoplasmic leaflet of the lipid bilayer. van Meer has estimated that the outer leaflet of the apical domain may consist almost entirely of glycolipids and cholesterol (56). If true, then hemagglutinin might be immersed in a sea of glycolipids during transport from the *trans*-Golgi to the plasma membrane. Upon extraction with Triton, lipid–protein complexes might precipitate. This hypothesis is encouraged by results from other cell types. In erythrocytes, sphingomyelin, which like glycolipids is derived from sphingosine, is insoluble in Triton X-100 at the ionic strength used in the present studies (63). In addition, ganglioside GM_1 associated with cholera toxin is insoluble in Triton (15, 53).

Changes in an Hemagglutinin Disulfide Bond

HA2 was lost from the immunoprecipitates of insoluble hemagglutinin which had been trypsin cleaved into HA1 and HA2 and denatured with SDS. This observation suggested that the disulfide bond linking HA1 and HA2 was not intact before immunoprecipitation. Protein disulfide bonds may be broken by reduction either by reaction with molecules like glutathione, which is present in high concentrations in the cell, or by disulfide exchange with cysteines of another protein. In the experiments described here, artifactual reduction of hemagglutinin disulfide bonds during extraction of cells is unlikely. Reactions in an air atmosphere (the conditions of these experiments), are invariably oxidizing rather than reducing. In addition, inclusion of sulfhydryl alkylating agents in the extraction solution, which might limit both disulfide exchange reactions and modify any reduced glutathione or other reductant, did not prevent loss of HA2. Since the loss of HA2 can be explained by reduction of the disulfide bond linking HA1 and HA2, this event may occur as part of the normal processing of hemagglutinin during intracellular transport.

The recovery of HA2 from pulse-labeled cells permeabilized, trypsinized, and extracted under denaturing conditions at different stages of transport demonstrated that although the disulfide bond linking HA1 and HA2 was formed during or soon after synthesis of the polypeptide chain, it was apparently reduced during transport. The results of this experiment are in partial agreement with similar data reported by Copeland et al. (7). They also found that the disulfide bond between HA1 and HA2 formed early in transport before trimerization. In their study they did not, however, detect breakage of this bond later in transport. This may not be a discrepancy with the results reported here. Copeland et al. extracted cells with Triton X-100 in PBS and discarded the insoluble pellet (7). If the hemagglutinin in this pellet had altered disulfide bonds, then this would have been missed (see below).

The observation that the disulfide bond linking HA1 and HA2 is formed initially but is later broken raises the possibility that a specific cellular activity is responsible for disrupting the disulfide bond. While no direct data to support this idea has been presented here, this hypothesis is most intriguing. In the H3 subtype of hemagglutinin for which the three-dimensional structure of the trimer is available, the disulfide bond between HA1 and HA2 is present near the membrane on the exoplasmic side (61). It has been shown that reduction of this bond in native hemagglutinin in vitro is not possible in the absence of acid-induced conformational changes (12, 61). On this basis, it seems reasonable to postulate that cellular reduction of the HA1/HA2 disulfide bond might require a conformational change or may occur as part of a process mediating a conformational change of the molecule.

Such an hypothesis was first proposed by Morrison et al. in their study of the fusion protein of Newcastle disease virus (26). They reported that during intracellular transport, the fusion protein undergoes a conformational change. When the protein was run on nonreducing gels, the early form ran with a mobility different from that of the protein fully reduced with mercaptoethanol. At later times, the mobility resembled that of the chemically reduced protein, suggesting that the protein had been reduced by the cell during transport.

Hemagglutinin Insolubility, Transport, and Sorting

Hemagglutinin becomes insoluble in polarized epithelial cells such as MDCK cells and LLC-PK1 cells, as well as in depolarized MDCK cells cultured in suspension and nonpolar cells like CEF and CV-1 cells (unpublished observations). It is evident, therefore, that insolubility and membrane polarity are not closely linked. What is the relationship, however, between sorting and polarity on the one hand, and insolubility and sorting on the other? Sorting is certainly a prerequisite for membrane polarity. Membrane polarity, though, depends also on the ability of the cell to maintain a polar distribution initially created by sorting. It is possible that all cells, polar and nonpolar as well, use similar mechanisms to deliver and insert proteins into the plasma membrane, and do so in a particular part of the plasma membrane. Migrating fibroblasts, for example, insert newly synthesized proteins in the leading edge (51). In AtT-20 and PC-12 cells, newly made secretory proteins accumulate at growing processes and along the midbody of dividing cells, clearly in a nonrandom fashion (24, 45, 54, 57). In epithelial cells, the apical surface may be akin to the fibroblast leading edge, with the exception that proteins inserted there can no longer diffuse to other parts of the surface because of persistent cytoskeletal interactions and the presence of junctional complexes. In this hypothesis, membrane traffic to other parts of the plasma membrane, the basolateral domain in epithelial cells, and regions other than the leading edge in fibroblasts, is not precluded. What is implied, though, is that this

transport occurs with mechanisms distinct from that directed to the leading edge or apex of the cell.

If sorting is merely the expression of a particular type of intracellular transport in the very specialized epithelial cell, then hemagglutinin insolubility may represent complex formation between the hemagglutinin and glycolipids, other membrane proteins, and possibly the cytoskeleton. Formation of such a complex may be essential primarily for getting the protein to the cell surface, but may also help to insure that the hemagglutinin, or other apical proteins, stay where they are delivered.

The authors thank Velia Fowler, Brian Burke, Cora-Ann Schoenenberger, and Robert Skibbens for helpful discussion and for critically reading the manuscript. We thank Donna Kendall for technical support and Betty Martindale for photography. We also thank J. Yewdell, W. Gerhard, and M.-J. Gething for providing antibodies.

This work was supported by grants from the National Institutes of Health to K. S. Matlin and M. G. Roth.

Received for publication 24 August 1988 and in revised form 2 November 1988.

Note Added in Proof: When the Triton-insoluble pellet derived from MDCK cells chased for 60 min was extracted with SDS at 0°C instead of at 95°C, the amount of hemagglutinin recovered was ~56% of the total instead of 26% as originally reported in this paper.

References

1. Balcarova-Stander, J., S. E. Pfeiffer, S. D. Fuller, and K. Simons. 1984. Development of cell surface polarity in the epithelial Madin-Darby canine kidney (MDCK) cell line. *EMBO (Eur. Mol. Biol. Organ.) J.* 3:2687–2694.
2. Deleted in press.
3. Bennett, V. 1982. The molecular basis of membrane-cytoskeleton association in human erythrocytes. *J. Cell. Biochem.* 18:49–65.
4. Bre, M.-H., T. E. Kreis, and E. Karsenti. 1987. Control of microtubule nucleation and stability in Madin–Darby canine kidney cells: the occurrence of noncentrosomal, stable detyrosinated microtubules. *J. Cell Biol.* 105:1283–1296.
5. Burke, B., K. Matlin, E. Bause, G. Legler, N. Peyrieras, and H. Ploegh. 1984. Inhibition of N-linked oligosaccharide trimming does not interfere with surface expression of certain integral membrane proteins. *EMBO (Eur. Mol. Biol. Organ.) J.* 3:551–556.
6. Caplan, M. J., H. C. Anderson, G. E. Palade, and J. D. Jamieson. 1986. Intracellular sorting and polarized cell surface delivery of (Na+,K+) ATPase, an endogenous component of MDCK cell basolateral plasma membranes. *Cell.* 46:623–631.
7. Copeland, C. S., K.-P. Zimmer, K. R. Wagner, G. A. Healey, I. Mellman, and A. Helenius. 1988. Folding, trimerization and transport are sequential events in the biogenesis of influenza virus hemagglutinin. *Cell.* 53: 197–209.
8. Fuhrman, U., E. Bause, G. Legler, and H. Ploegh. 1984. Novel mannosidase inhibitor blocking conversion of high mannose to complex oligosaccharides. *Nature (Lond.).* 307:755–758.
9. Fuller, S. D., R. Bravo, and K. Simons. 1985. An enzymatic assay reveals that proteins destined for the apical or the basolateral domains of an epithelial cell line share the same late Golgi compartments. *EMBO (Eur. Mol. Biol. Organ.) J.* 4:297–307.
10. Gaush, C. R., W. L. Hard, and T. F. Smith. 1966. Characterization of an established line of Canine Kidney Cells (MDCK). *Proc. Soc. Exp. Biol. Med.* 122:931–936.
11. Gottlieb, T. A., G. Beaudry, L. Rizzolo, A. Colman, M. Rindler, M. Adesnik, and D. D. Sabatini. 1986. Secretion of endogenous and exogenous proteins from polarized MDCK cell monolayers. *Proc. Natl. Acad. Sci. USA.* 83:2100–2104.
12. Graves, P. N., J. L. Schulman, J. F. Young, and P. Palese. 1983. Preparation of influenza virus subviral particles lacking the HA1 subunit of hemagglutinin: unmasking of cross-reactive HA2 determinants. *Virology.* 126:106–116.
13. Griffiths, G., and K. Simons. 1986. The *trans* Golgi network: sorting at the exit site of the Golgi complex. *Science (Wash. DC).* 234:438–443.
14. Griffiths, G., S. Pfeiffer, K. Simons, and K. Matlin. 1985. Exit of newly synthesized membrane proteins from the *trans*-cisterna of the Golgi complex to the plasma membrane. *J. Cell Biol.* 101:949–964.
15. Hagmann, J., and P. H. Fishman. 1982. Detergent extraction of cholera toxin and gangliosides from cultured cells and isolated membranes. *Biochim. Biophys. Acta.* 720:181–187.
16. Kelly, R. B. 1985. Pathways of protein secretion in eukaryotes. *Science (Wash. DC).* 230:25–32.
17. Klenk, H.-D., R. Rott, M. Ohlich, and J. Blodom. 1975. Activation of influenza A viruses by trypsin treatment. *Virology.* 68:426–439.
18. Kondor-Koch, C., R. Bravo, S. D. Fuller, D. Cutler, and H. Garoff. 1985. Protein secretion in the polarized epithelial cell line MDCK. *Cell.* 43: 297–306.
19. Lazarowitz, S. G., and P. W. Choppin. 1975. Enhancement of the infectivity of influenza A and B viruses by proteolytic cleavage of the hemagglutinin polypeptide. *Virology.* 68:440–454.
20. Matlin, K. S., and K. Simons. 1983. Reduced temperature prevents transfer of a membrane glycoprotein to the cell surface but does not prevent terminal glycosylation. *Cell.* 34:233–243.
21. Matlin, K. S., and K. Simons. 1984. Sorting of an apical plasma membrane glycoprotein occurs before it reaches the cell surface in cultured epithelial cells. *J. Cell Biol.* 99:2131–2139.
22. Matlin, K. S., H. Reggio, A. Helenius, and K. Simons. 1981. Infectious entry pathway of influenza virus in a canine kidney cell line. *J. Cell Biol.* 91:601–613.
23. Matlin, K. S., J. Skibbens, and P. L. McNeil. 1988. Reduced extracellular pH reversibly inhibits oligomerization, intracellular transport and processing of influenza hemagglutinin in infected Madin-Darby canine kidney cells. *J. Biol. Chem.* 263:11478–11485.
24. Matsuuchi, L., K. M. Buckley, A. W. Lowe, and R. B. Kelly. 1988. Targeting of secretory vesicles to cytoplasmic domains in AtT-20 and PC-12 cells. *J. Cell Biol.* 106:239–252.
25. Misek, D. E., E. Bard, and E. Rodriguez-Boulan. 1984. Biogenesis of epithelial cell polarity: intracellular sorting and vectorial exocytosis of an apical plasma membrane glycoprotein. *Cell.* 39:537–546.
26. Morrison, T. G., M. E. Peeples, and L. W. McGinnes. 1987. Conformational change in a viral glycoprotein during maturation due to disulfide bond disruption. *Proc. Natl. Acad. Sci. USA.* 84:1020–1024.
27. Nelson, W. J., and R. W. Hammerton. 1989. A membrane–cytoskeletal complex containing Na^+,K^+-ATPase, ankyrin, and fodrin in Madin–Darby canine kidney cells: implications for the biogenesis of epithelial cell polarity. *J. Cell Biol.* 108:893–902.
28. Nelson, W. J., and P. J. Veshnock. 1986. Dynamics of membrane-skeleton (fodrin) organization during development of polarity in Madin–Darby canine kidney epithelial cells. *J. Cell Biol.* 103:1751–1765.
29. Nelson, W. J., and P. J. Veshnock. 1987. Modulation of fodrin (membrane skeleton) stability by cell–cell contact in Madin–Darby canine kidney epithelial cell. *J. Cell Biol.* 104:1527–1537.
30. Nelson, W. J., and P. J. Veshnock. 1987. Ankyrin binding to Na^+/K^+-ATPase and implications for the organization of membrane domains. *Nature (Lond.).* 328:533–536.
31. Nigg, E. A., G. Schafer, H. Hilz, and H. M. Eppenberger. 1985. Cyclic-AMP-dependent protein kinase type II is associated with the Golgi complex and with centrosomes. *Cell.* 41:1039–1051.
32. Novikoff, A. B. 1976. The endoplasmic reticulum: a cytochemist's view (a review). *Proc. Natl. Acad. Sci. USA.* 73:2781–2787.
33. Orci, L., P. Halban, M. Amherdt, M. Ravazzola, J. D. Vassalli, and A. Perrelet. 1984. A clathrin-coated, Golgi-related compartment of the insulin secreting cell accumulates proinsulin in the presence of monensin. *Cell.* 39:39–47.
34. Orci, L., M. Ravazzola, M. Amherdt, D. Louvard, and A. Perrelet. 1985. Clathrin-immunoreactive site in the Golgi apparatus are concentrated at the *trans* pole in polypeptide hormone-secreting cells. *Proc. Natl. Acad. Sci. USA.* 82:5385–5389.
35. Orci, L., M. Ravazzola, M. Amherdt, A. Perrelet, S. K. Powell, D. L. Quinn, and H.-P. H. Moore. 1987. The *trans*-most cisternae of the Golgi complex: a compartment for sorting of secretory and plasma membrane proteins. *Cell.* 51:1039–1051.
36. Pfeiffer, S., S. D. Fuller, and K. Simons. 1985. Intracellular sorting and basolateral appearance of the G protein of vesicular stomatitis virus in MDCK cells. *J. Cell Biol.* 101:470–476.
37. Piccioni, R., G. Bellemare, and N.-H. Chua. 1982. Methods of polyacrylamide gel electrophoresis in the analysis and preparation of plant polypeptides. *In* Methods in Chloroplast Molecular Biology. M. Edelman, R. B. Hallich, and N.-H. Chua, editors. Elsevier/North Holland, Amsterdam. 985–1014.
38. Rabito, C.A., and M. V. Karish. 1982. Polarized amino acid transport by an epithelial cell line of renal origin (LLC-PK1). *J. Biol. Chem.* 257: 6802–6808.
39. Rindler, M. J., I. E. Ivanov, H. Plesken, E. Rodriguez-Boulan, and D. D. Sabatini. 1984. Viral glycoproteins destined for apical or basolateral plasma membrane domains traverse the same Golgi apparatus during their intracellular transport in doubly infected Madin–Darby canine kidney cells. *J. Cell Biol.* 98:1304–1319.
40. Rindler, M. J., I. E. Ivanov, H. Plesken, and D. D. Sabatini. 1985. Polarized delivery of viral glycoproteins to the apical and basolateral plasma membranes of Madin–Darby canine kidney cells infected with temperature-sensitive viruses. *J. Cell Biol.* 100:136–151.
41. Rindler, M. J., I. E. Ivanov, and D. D. Sabatini. 1987. Microtubule-acting drugs lead to the nonpolarized delivery of influenza hemagglutinin to the

cell surface of polarized Madin-Darby canine kidney cells. *J. Cell Biol.* 104:231-241.
42. Rodriguez-Boulan, E., and M. Pendergast. 1980. Polarized distribution of viral envelope glycoproteins in the plasma membrane of infected epithelial cells. *Cell.* 20:45-54.
43. Rodriguez-Boulan, E., and D. D. Sabatini. 1978. Asymmetric budding of viruses in epithelial monolayers: a model system for study of epithelial polarity. *Proc. Natl. Acad. Sci. USA.* 75:5071-5075.
44. Rodriguez-Boulan, E., K. T. Paskiet, and D. D. Sabatini. 1983. Assembly of enveloped viruses in Madin-Darby canine kidney cells: polarized budding from single attached cells and from clusters of cells in suspension. *J. Cell Biol.* 96:866-874.
45. Rogalski, A. A., J. E. Bergmann, and S. Singer. 1984. Effect of microtubule assembly status on the intracellular processing and surface expression of an integral protein of the plasma membrane. *J. Cell Biol.* 99: 1101-1109.
46. Roth, M. G., M.-J. Gething, J. Sambrook, L. Giusti, A. Davis, D. Nayak, and R. W. Compans. 1983. Influenza virus hemagglutinin expression is polarized in cells infected with recombinant SV40 viruses carrying cloned hemagglutinin DNA. *Cell.* 33:435-443.
47. Salas, P. J. I., D. E. Misek, D. E. Vega-Salas, D. Gundersen, M. Cereijido, and E. Rodriguez-Boulan. 1986. Microtubules and actin filaments are not critically involved in the biogenesis of epithelial cell surface polarity. *J. Cell Biol.* 102:1853-1867.
48. Sambrook, J., L. Rodgers, J. White, and M.-J. Gething. 1985. Lines of BPV-transformed murine cells that constitutively express influenza virus hemagglutinin. *EMBO (Eur. Mol. Biol. Organ.) J.* 4:91-103.
49. Sheetz, M. P. 1979. Integral membrane protein interaction with Triton cytoskeletons of erythrocytes. *Biochim. Biophys. Acta.* 557:122-134.
50. Simons, K., and S. D. Fuller. 1985. Cell surface polarity in epithelia. *Annu. Rev. Cell Biol.* 1:243-288.
51. Singer, S. J., and A. Kupfer. 1986. The directed migration of eukaryotic cells. *Annu. Rev. Cell Biol.* 2:337-365.
52. Stephens, E. B., R. W. Compans, P. Earl, and B. Moss. 1986. Surface expression of viral glycoproteins in polarized epithelial cells infected with recombinant vaccinia viral vectors. *EMBO (Eur. Mol. Biol. Organ.) J.* 5:237-245.
53. Streuli, C. H., B. Patel, and D. R. Critchley. 1981. The cholera toxin receptor ganglioside GM1 remains associated with Triton X-100 cytoskeletons of BALB/c-3T3 cells. *Exp. Cell Res.* 136:247-254.
54. Tooze, J., and B. Burke. 1987. Accumulation of adrenocorticotropin secretory granules in the midbody of telophase AtT-20 cells: evidence that secretory granules move anterogradely along microtubules. *J. Cell Biol.* 104:1047-1057.
55. Tooze, J., and S. A. Tooze. 1986. Clathrin-coated vesicular transport of secretory proteins during the formation of ACTH-containing secretory granules in AtT-20 cells. *J. Cell Biol.* 103:839-850.
56. van Meer, G. 1988. How epithelia grease their microvilli. *Trends Biochem. Sci.* 13:242-243.
57. van Meer, G., and K. Simons. 1982. Viruses budding from either the apical or the basolateral plasma membrane domain of MDCK cells have unique phospholipid compositions. *EMBO (Eur. Mol. Biol. Organ.) J.* 7:847-852.
58. van Meer, G., and K. Simons. 1986. The function of tight junctions in maintaining differences in lipid composition between the apical and basolateral cell surface domains of MDCK cells. *EMBO (Eur. Mol. Biol. Organ.) J.* 5:1455-1464.
59. van Meer, G., E. H. K. Stelzer, R. W. Wijnaendts-van-Resandt, and K. Simons. 1987. Sorting of sphingolipids in epithelial (Madin-Darby canine kidney) cells. *J. Cell Biol.* 105:1623-1636.
60. Walter, P., R. C. Jackson, M. M. Marcus, V. R. Lingappa, and G. Blobel. 1979. Tryptic dissection and reconstitution of translocation activity for nascent presecretory proteins across microsomal membranes. *Proc. Natl. Acad. Sci. USA.* 76:1795-1799.
61. Wiley, D. C., and J. J. Skehel. 1987. The structure and function of the hemagglutinin membrane glycoprotein of influenza virus. *Annu. Rev. Biochem.* 56:365-394.
62. Winter, G., S. Fields, and G. G. Brownlee. 1981. Nucleotide sequence of the hemagglutinin gene of a human influenza virus H1 subtype. *Nature (Lond.).* 292:72-75.
63. Yu, J., D. A. Fischman, and T. L. Steck. 1973. Selective solubilization of proteins and phospholipids from red blood cell membranes by nonionic detergents. *J. Supramol. Struct.* 3:233-248.